Single and double ionization in C⁶⁺ + He collisions

M. S. Pindzola and F. Robicheaux

Department of Physics, Auburn University, Auburn, Alabama 36849, USA

J. Colgan

Theoretical Division, Los Alamos National Laboratory, Los Alamos, New Mexico 87545, USA
(Received 10 August 2010; published 26 October 2010)

Single- and double-ionization processes in C⁶⁺ collisions with the He atom at an incident energy of 100 MeV/amu are studied by direct solution of the time-dependent Schrödinger equation. A time-dependent close-coupling method based on an expansion of a one-electron three-dimensional wave function in the field of He⁺ is used to calculate single-ionization cross sections. A time-dependent close-coupling method based on an expansion of a two-electron six-dimensional wave function in the field of He²⁺ is used to calculate single- and double-ionization cross sections. Electron energy and angle differential cross sections for single ionization are presented for various projectile impact parameters. For relatively large impact parameters, the differential cross sections are in qualitative agreement with ion-atom experiments. Electron energy and angle differential cross sections for double ionization are also presented for a relatively large projectile impact parameter.

I. INTRODUCTION

The collision of fast bare ions with atoms provides an interesting probe of various electron ionization processes. Under photon impact, the electrons feel a dipolar interaction for a fixed intensity, while for a fast bare ion impact the electrons feel a multipolar interaction that varies with ion-atom impact distance. From a theoretical perspective, the single and double ionization of atoms by fast bare ion impact are challenging many-body quantal breakup problems.

In the past few years a nonperturbative time-dependent close-coupling (TDCC) method has been developed and applied to various ion-atom and ion-molecule collisions. For single and double ionization in α + He collisions from 1.0 to 1.6 MeV/amu, the TDCC results [1] were found to be in good agreement with basis-set coupled-channels calculations [2] and experiments [3,4] for total cross sections. For single and double ionization in $\bar{p}$ + He collisions from 0.01 to 1.0 MeV/amu, the TDCC results [5] for total cross sections were found to be in good agreement with time-dependent flatland lattice calculations [6] and experiment [7] for single ionization, as well as in good agreement with experiment [7] for double ionization. For double ionization in p + He collisions at 6.0 MeV/amu, the TDCC results [8] were found to be in good relative agreement with experiment [9] for the double-angle differential cross section. Finally, for single and double ionization in p + H₂ collisions at 1.0 MeV/amu, the TDCC results [10] were found to be in good agreement with experiments [11,12] for the double to single cross-section ratio.

In this article, we use the TDCC method to calculate the single ionization in C⁶⁺ + He collisions at 100 MeV/amu to compare with the pioneering experiments of Schulz *et al.* [13], which measured differential cross sections in electron energy, electron angle, and projectile angle. We first apply a TDCC method based on an expansion of a one-electron three-dimensional (3D) wave function in the field of He⁺ to calculate electron energy and angle differential cross sections for single ionization at various projectile impact parameters. We then apply a TDCC method based on an expansion of a

two-electron six-dimensional (6D) wave function in the field of He²⁺ to check our TDCC-3D single-ionization differential cross-section results. Finally, we use the TDCC-6D method to calculate electron energy and angle differential cross sections for double ionization at a relatively large projectile impact parameter to guide future C⁶⁺ + He collision experiments.

In the experiments of Schulz *et al.* [13], the "perturbation" of the incoming projectile, related to the projectile charge over the projectile velocity, is small and in such a perturbative regime one expects that a first Born approximation should be reasonable for all single-ionization cross sections. This was found to be the case for the differential cross sections in the coplanar geometry, where theory and experiment are in very good agreement [14], but not for the perpendicular plane geometry. In the perpendicular plane, differential cross-section measurements found a double-hump structure, whereas first Born and distorted-wave treatments found an almost flat isotropic distribution. These findings initiated many sets of theoretical studies. For example, later studies [15] showed that an improved treatment of the electron-ion interactions had little effect on the distorted-wave calculations, and it was shown that the agreement between experiment and theory grew steadily worse as one moves from the coplanar to the perpendicular plane. A very recent study using an impact-parameter coupled-pseudostate approximation [16] reported similar results to the earlier distorted-wave calculations, which is in good agreement with measurement in the coplanar geometry but poor agreement in the perpendicular plane. Other studies have asserted that the disagreement in the perpendicular plane is due to issues with the experimental resolution [17], although this explanation has been refuted [18]. Alternative explanations for the differences between experiment and theory in terms of elastic scattering of the projectile by the He nucleus have also been put forward [19].

The rest of the article is organized as follows. In Sec. II A we present a TDCC-3D method for calculating fully differential cross sections for the single ionization of atoms with one active electron, in Sec. II B we present a TDCC-6D method

for calculating fully differential cross sections for the single and double ionization of atoms with two active electrons, and in Sec. II C we review the relation between projectile impact parameter and projectile scattering angle. In Sec. III we apply the TDCC-3D and TDCC-6D methods to calculate fully differential cross sections for single and double ionization in C^{6+} + He collisions at 100.0 MeV/amu to compare with experiment. In Sec. IV, we conclude with a summary and an outlook for future work. Unless otherwise stated, all quantities are given in atomic units.

II. THEORY

A. 3D time-dependent close-coupling method

For single ionization in fast bare ion collisions with atoms with one active electron, we solve the time-dependent Schrödinger equation,

$$i \frac{\partial \Psi(\vec{r},t)}{\partial t} = H_{\text{system}} \Psi(\vec{r},t), \tag{1}$$

where the nonrelativistic Hamiltonian is given by

$$H_{\text{system}} = -\frac{1}{2} \nabla^2 - \frac{Z_t}{r} + V(r) - \frac{Z_p}{|\vec{r} - \vec{R}(t)|}, \tag{2}$$

where Z_t is the target atomic number, $V(r)$ is a Hartree-local exchange potential for the atomic core, and Z_p is the projectile atomic number. For straight-line motion in the target frame of reference, which ignores the projectile-target interaction, the magnitude of the time-dependent projectile position is given by

$$R(t) = \sqrt{b^2 + (d_0 + vt)^2}, \tag{3}$$

where b is an impact parameter, d_0 is a starting distance, and v is the projectile speed.

If we expand $\Psi(\vec{r},t)$ in spherical harmonics,

$$\Psi(\vec{r},t) = \sum_{l,m} \frac{P_{lm}(r,t)}{r} Y_{lm}(\theta,\phi), \tag{4}$$

the resulting close-coupled equations for the $P_{lm}(r,t)$ radial expansion functions are given by

$$i \frac{\partial P_{lm}(r,t)}{\partial t} = T_l(r) P_{lm}(r,t) + \sum_{l',m'} W_{lm,l'm'}(r,R(t)) P_{l'm'}(r,t), \tag{5}$$

where

$$T_l(r) = -\frac{1}{2} \frac{\partial^2}{\partial r^2} + \frac{l(l+1)}{2r^2} - \frac{Z_t}{r} + V_l(r). \tag{6}$$

The electron-projectile coupling operator is given by

$$W_{lm,l'm'}(r,R(t))$$
$$= -Z_p \sum_{\lambda} \frac{(r,R(t))_<^{\lambda}}{(r,R(t))_>^{\lambda+1}} \sum_q C_q^{\lambda*}(\theta_p,\phi_p)(-1)^m$$
$$\times \sqrt{(2l+1)(2l'+1)} \begin{pmatrix} l & \lambda & l' \\ 0 & 0 & 0 \end{pmatrix} \begin{pmatrix} l & \lambda & l' \\ -m & q & m' \end{pmatrix}, \tag{7}$$

where λ,q are multipole expansion coefficients. For projectile motion in the xz plane with d_0 along the z axis, the spherical tensor is given by

$$C_q^{\lambda}(\theta_p,\phi_p) = \sqrt{\frac{4\pi}{2\lambda+1}} Y_{\lambda q}(\theta_p,0), \tag{8}$$

where $\sin\theta_p = b/R(t)$ and $\cos\theta_p = (d_0 + vt)/R(t)$.

The initial condition for the solution of the TDCC-3D equations for single ionization of the ground state of He is given by

$$P_{lm}(r,t=0) = P_{1s}(r)\delta_{l,0}\delta_{m,0}, \tag{9}$$

where $P_{1s}(r)$ is a bound radial orbital obtained by diagonalization of the Hamiltonian:

$$H(r) = -\frac{1}{2} \frac{\partial^2}{\partial r^2} - \frac{2}{r} + V_l(r). \tag{10}$$

Following the time propagation of the TDCC-3D equations, momentum-space wave functions at various impact parameters are calculated by

$$P_{lm}(b,k) = \int_0^\infty dr\, P_{kl}(r) \bar{P}_{lm}(r,t \to \infty), \tag{11}$$

where

$$\bar{P}_{lm}(r,t \to \infty) = P_{lm}(r,t \to \infty) - \alpha P_{1s}(r)\delta_{l,0}\delta_{m,0}, \tag{12}$$

$$\alpha = \int_0^\infty dr\, P_{1s}(r) P_{00}(r,t \to \infty), \tag{13}$$

and $P_{kl}(r)$ is a box normalized continuum distorted-wave. The fully differential cross section for the single ionization of the ground state of He is given by

$$\frac{d^4\sigma}{db\,dk\,d\theta\,d\phi} = 2 \left| \sum_{l,m} (-i)^l e^{i(\sigma_l+\delta_l)} P_{lm}(b,k) Y_{lm}(\theta,\phi) \right|^2, \tag{14}$$

where the factor of 2 is the occupation number of the $1s$ subshell, σ_l is a Coulomb phase shift, and δ_l is a distorted-wave phase shift due to the $V_l(r)$ potential. The total cross section is obtained by integration over electron scattering solid angle, electron momentum, and projectile impact parameter given by

$$\sigma = 2\pi \int_0^\infty b\,db \int_0^\infty dk \int_0^\pi \sin\theta\,d\theta \int_0^{2\pi} d\phi \frac{d^4\sigma}{db\,dk\,d\theta\,d\phi}. \tag{15}$$

As for all differential cross sections, the units are area divided by the units of all the differential quantities. The differential cross section of Eq. (14) has the units of area divided by length squared for $2\pi b\,db$ times momentum for dk times solid angle for $\sin\theta\,d\theta\,d\phi$. In addition, we multiply our differential cross sections by 2.8×10^7 such that the total cross sections are in barns (1.0×10^{-24} cm^2).

B. 6D time-dependent close-coupling method

For single and double ionization in fast bare ion collisions with atoms with two active electrons, we solve the

time-dependent Schrödinger equation,

$$i\frac{\partial\Psi(\vec{r}_1,\vec{r}_2,t)}{\partial t} = H_{\text{system}}\Psi(\vec{r}_1,\vec{r}_2,t), \qquad (16)$$

where the nonrelativistic Hamiltonian is given by

$$H_{\text{system}} = \sum_{i=1,2}\left(-\frac{1}{2}\nabla_i^2 - \frac{Z_t}{r_i} + V(r_i)\right)$$
$$+ \frac{1}{|\vec{r}_1-\vec{r}_2|} - \sum_{i=1,2}\frac{Z_p}{|\vec{r}_i-\vec{R}(t)|}. \qquad (17)$$

If we expand $\Psi(\vec{r}_1,\vec{r}_2,t)$ in coupled spherical harmonics,

$$\Psi(\vec{r}_1,\vec{r}_2,t) = \sum_{l_1,l_2}\frac{P_{l_1l_2}^{LM}(r_1,r_2,t)}{r_1r_2}\sum_{m_1,m_2}C_{m_1m_2M}^{l_1l_2L}$$
$$\times Y_{l_1m_1}(\theta_1,\phi_1)Y_{l_2m_2}(\theta_2,\phi_2), \qquad (18)$$

the resulting close-coupled equations for the $P_{l_1l_2}^{LM}(r_1,r_2,t)$ radial expansion functions are given by [1]

$$i\frac{\partial P_{l_1l_2}^{LM}(r_1,r_2,t)}{\partial t}$$
$$= T_{l_1l_2}(r_1,r_2)P_{l_1l_2}^{LM}(r_1,r_2,t)$$
$$+ \sum_{l_1',l_2'}V_{l_1l_2,l_1'l_2'}^{L}(r_1,r_2)P_{l_1'l_2'}^{LM}(r_1,r_2,t)$$
$$+ \sum_{L',M'}\sum_{l_1',l_2'}W_{l_1l_2,l_1'l_2'}^{LM,L'M'}(r_1,R(t))P_{l_1'l_2'}^{L'M'}(r_1,r_2,t)$$
$$+ \sum_{L',M'}\sum_{l_1',l_2'}W_{l_1l_2,l_1'l_2'}^{LM,L'M'}(r_2,R(t))P_{l_1'l_2'}^{L'M'}(r_1,r_2,t), \qquad (19)$$

where

$$T_{l_1l_2}(r_1,r_2) = \sum_{i=1,2}\left(-\frac{1}{2}\frac{\partial^2}{\partial r_i^2} + \frac{l_i(l_i+1)}{2r_i^2} - \frac{Z_t}{r_i} + V_{l_i}(r_i)\right). \qquad (20)$$

The electron-electron coupling operator is given by

$$V_{l_1l_2,l_1'l_2'}^{L}(r_1,r_2)$$
$$= (-1)^{L+l_2+l_2'}\sqrt{(2l_1+1)(2l_1'+1)(2l_2+1)(2l_2'+1)}$$
$$\times \sum_{\lambda}\frac{(r_1,r_2)_<^{\lambda}}{(r_1,r_2)_>^{\lambda+1}}\begin{pmatrix}l_1 & \lambda & l_1' \\ 0 & 0 & 0\end{pmatrix}\begin{pmatrix}l_2 & \lambda & l_2' \\ 0 & 0 & 0\end{pmatrix}\begin{Bmatrix}L & l_2' & l_1' \\ \lambda & l_1 & l_2\end{Bmatrix}. \qquad (21)$$

The electron-projectile coupling operators are given by

$$W_{l_1l_2,l_1'l_2'}^{LM,L'M'}(r_1,R(t))$$
$$= -Z_p\delta_{l_2,l_2'}(-1)^{l_2+L+L'-M}$$
$$\times \sqrt{(2l_1+1)(2l_1'+1)(2L+1)(2L'+1)}$$
$$\times \sum_{\lambda}(-1)^{\lambda}\frac{(r_1,R(t))_<^{\lambda}}{(r_1,R(t))_>^{\lambda+1}}\begin{pmatrix}l_1 & \lambda & l_1' \\ 0 & 0 & 0\end{pmatrix}$$
$$\times \sum_q C_q^{\lambda*}(\theta_p,\phi_p)\begin{pmatrix}L & \lambda & L' \\ -M & q & M'\end{pmatrix}\begin{Bmatrix}l_1 & l_2 & L \\ L' & \lambda & l_1'\end{Bmatrix}, \qquad (22)$$

and

$$W_{l_1l_2,l_1'l_2'}^{LM,L'M'}(r_2,R(t))$$
$$= -Z_p\delta_{l_1,l_1'}(-1)^{l_1+l_2+l_2'-M}$$
$$\times \sqrt{(2l_2+1)(2l_2'+1)(2L+1)(2L'+1)}$$
$$\times \sum_{\lambda}(-1)^{\lambda}\frac{(r_2,R(t))_<^{\lambda}}{(r_2,R(t))_>^{\lambda+1}}\begin{pmatrix}l_2 & \lambda & l_2' \\ 0 & 0 & 0\end{pmatrix}$$
$$\times \sum_q C_q^{\lambda*}(\theta_p,\phi_p)\begin{pmatrix}L & \lambda & L' \\ -M & q & M'\end{pmatrix}\begin{Bmatrix}l_1 & l_2 & L \\ \lambda & L' & l_2'\end{Bmatrix}. \qquad (23)$$

The initial condition for the solution of the TDCC-6D equations for single and double ionization of the ground state of He is given by

$$P_{l_1l_2}^{LM}(r_1,r_2,t=0) = \sum_l \hat{P}_{ll}^{00}(r_1,r_2)\delta_{l_1,l}\delta_{l_2,l}\delta_{L,0}\delta_{M,0}, \qquad (24)$$

where the radial wave functions, $\hat{P}_{ll}^{00}(r_1,r_2)$, are obtained by relaxation of the TDCC-6D equations with no electron-projectile coupling operators in imaginary time.

Following the time propagation of the TDCC-6D equations in real time, single-ionization momentum-space wave functions at various impact parameters are calculated by

$$P_{0L}^{LM}(b,k)$$
$$= \int_0^{\infty}dr_1\int_0^{\infty}dr_2 P_{1s}(r_1)P_{kL}(r_2)\bar{P}_{0L}^{LM}(r_1,r_2,t\to\infty), \qquad (25)$$

where

$$\bar{P}_{0L}^{LM}(r_1,r_2,t\to\infty)$$
$$= P_{0L}^{LM}(r_1,r_2,t\to\infty) - \beta\hat{P}_{00}^{00}(r_1,r_2)\delta_{L,0}\delta_{M,0}, \qquad (26)$$

$$\beta = \sum_l\int_0^{\infty}dr_1\int_0^{\infty}dr_2\hat{P}_{ll}^{00}(r_1,r_2)P_{ll}^{00}(r_1,r_2,t\to\infty), \qquad (27)$$

and $P_{kl}(r)$ is a box-normalized continuum Coulomb wave. The fully differential cross section for the single ionization of the ground state of He is given by

$$\frac{d^4\sigma}{db\,dk\,d\theta\,d\phi} = 2\left|\sum_{L,M}(-i)^L e^{i\sigma_L}P_{0L}^{LM}(b,k)Y_{LM}(\theta,\phi)\right|^2, \qquad (28)$$

where the factor of 2 comes from only projecting onto $1skl$ products. The total cross section is again obtained by integration over electron scattering solid angle, electron momentum, and projectile impact parameter.

Following the time propagation of the TDCC-6D equations in real time, double-ionization momentum-space wave functions at various impact parameters are given by

$$P_{l_1l_2}^{LM}(b,k_1,k_2)$$
$$= \int_0^{\infty}dr_1\int_0^{\infty}dr_2 P_{k_1l_1}(r_1)P_{k_2l_2}(r_2)\bar{P}_{l_1l_2}^{LM}(r_1,r_2,t\to\infty), \qquad (29)$$

where

$$\bar{P}_{l_1 l_2}^{LM}(r_1, r_2, t \to \infty)$$
$$= P_{l_1 l_2}^{LM}(r_1, r_2, t \to \infty) - \beta \hat{P}_{ll}^{00}(r_1, r_2)\delta_{l_1,l}\delta_{l_2,l}\delta_{L,0}\delta_{M,0}. \quad (30)$$

The fully differential cross section for the double ionization of the ground state of He is given by

$$\frac{d^7\sigma}{db\, dk_1\, dk_2\, d\theta_1\, d\theta_2\, d\phi_1\, d\phi_2}$$

$$= \left| \sum_{l_1,l_2} \sum_{L,M} (-i)^{l_1+l_2} e^{i(\sigma_{l_1}+\sigma_{l_2})} P_{l_1 l_2}^{LM}(b, k_1, k_2) \right.$$

$$\left. \times \sum_{m_1,m_2} C_{m_1 m_2 M}^{l_1 l_2 L} Y_{l_1 m_1}(\theta_1, \phi_1) Y_{l_2 m_2}(\theta_2, \phi_2) \right|^2. \quad (31)$$

The total cross section is obtained by integration over both electron scattering solid angles, both electron momenta, and projectile impact parameter.

C. Projectile scattering angle

From classical Rutherford scattering theory, a small-angle collision between a projectile ion with charge Z_p and a target ion with charge Z_t results in a total momentum transfer to the projectile given by

$$\Delta p = \frac{2Z_p Z_t}{vb}, \quad (32)$$

where v is the projectile speed and b is the impact parameter. A collision between a projectile ion with charge Z_p and a target atom with nuclear charge Z_t results in a total momentum transfer to the projectile given by

$$\Delta p = Z_p \int_0^\infty dt\, \frac{Q(t)b}{R(t)^3}, \quad (33)$$

where $Q(t)$ is a time-dependent average charge. Using the one-electron radial wave functions, $P_{lm}(r,t)$, from a TDCC-3D calculation for He, the average charge is given by

$$Q(t) = Z_t - 2.0 \sum_{l,m} \int_0^{R(t)} dr\, |P_{lm}(r,t)|^2, \quad (34)$$

where $Z_t = 2.0$. Since $Q(t)$ is calculated using all lm scattering channels it includes all elastic and inelastic processes. For a specific inelastic process, the range of momentum transfer to the projectile is approximately given by

$$\Delta p = \frac{2Z_p(Z_t - 1)}{vb} \pm \hat{k}, \quad (35)$$

where $\hat{k}$ is the momentum transferred to the electron by the projectile. Finally, the projectile scattering angle is given by

$$\Phi = \frac{\Delta p}{Mv}, \quad (36)$$

where M is the projectile mass.

III. RESULTS

We first use the TDCC-3D method to calculate single-ionization cross sections in C^{6+} + He collisions at 100 MeV/amu. We begin by diagonalizing the radial

Hamiltonian of Eq. (10), where our choice for the Hartree-local exchange potential is given by

$$V_l(r) = J_{1s}^0(r) - \frac{c_l}{2}\left(\frac{24\rho_{1s}}{\pi}\right)^{\frac{1}{3}}, \quad (37)$$

where $J_{nl}^\kappa(r)$ is the direct potential, ρ_{nl} is the probability density, and the $1s$ core wave function is the hydrogenic solution for He^+. On a 384-point uniform radial coordinate mesh with $\Delta r = 0.10$, a coefficient of $c_0 = 0.21$ gives a binding energy of -24.6 eV in agreement with experiment [20]. The $P_{1s}(r)$ bound orbital from the diagonalization is used in the initial condition of Eq. (9). Continuum orbitals are obtained by direct integration of the radial Schrödinger equation given by

$$H(r)P_{kl}(r) = \epsilon P_{kl}(r) \quad (38)$$

for 300 box-normalized functions with a uniform spacing of $\Delta k = 0.05$ to span an electron energy, $\epsilon = \frac{k^2}{2}$, up to 3 keV. The $P_{kl}(r)$ continuum orbitals are used to obtain momentum-space wave functions in Eq. (11).

The TDCC-3D cross-section results are obtained by time propagating Eq. (5) from $d_0 = -50$ to $d_{final} = +421$ at 30 different impact parameters. All 30 calculations used 16 lm close-coupled channels. The total cross section was found to be 1.49×10^{-17} cm^2, in reasonable agreement with a first Born approximation result of 1.29×10^{-17} cm^2 and a distorted-wave result of 1.44×10^{-17} cm^2 [14].

A principal finding of this article is that the differential cross section for single ionization in C^{6+} + He collisions at 100 MeV/amu dramatically evolves as a function of projectile impact parameter. The weighted differential cross section $b\frac{d\sigma}{db}$ increases to a peak at $b = 1.0$ and then tails off at higher impact parameters. As shown in Fig. 1, the shape of the $\phi = 0$ in plane differential cross section changes rapidly until about $b = 1.0$,
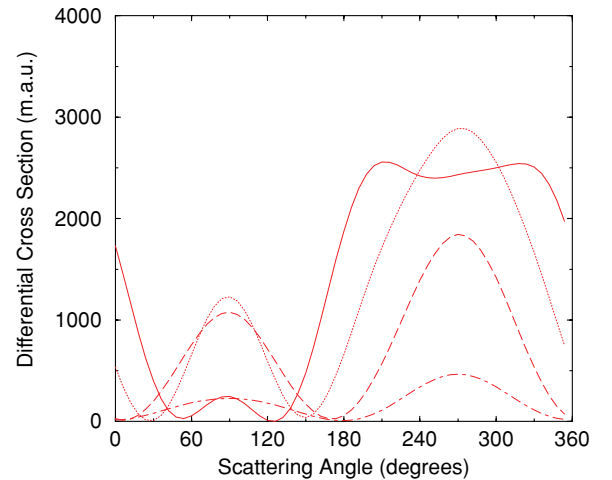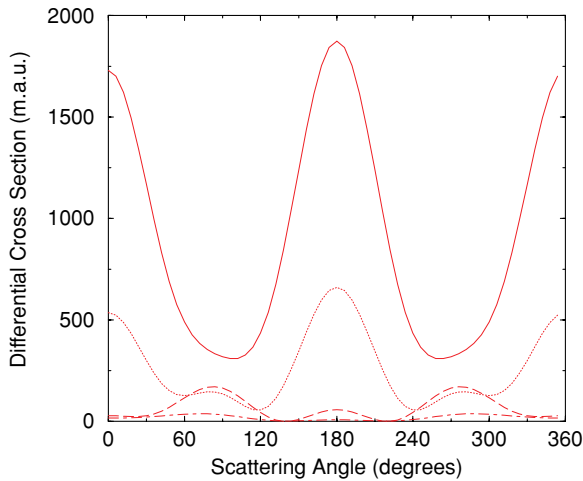

FIG. 1. (Color online) The differential cross section for single ionization in C^{6+} + He collisions at a projectile energy of 100 MeV/amu, an ejected-electron energy of $\epsilon = 6.67$ eV, $\phi = 0$, and $\theta = 0$–360. Solid curve, TDCC-3D calculation at $b = 0.5$; dotted curve, TDCC-3D calculation at $b = 1.0$; dashed curve, TDCC-3D calculation at $b = 2.0$; dot-dashed curve, TDCC-3D calculation at $b = 4.0$ (m.a.u. = modified atomic units equal to 2.8×10^7 times atomic units such that the total cross section is in units of 1.0×10^{-24} cm^2).

FIG. 2. (Color online) The differential cross section for single ionization in C^{6+} + He collisions at a projectile energy of 100 MeV/amu, an ejected electron energy of $\epsilon = 6.67$ eV, $\phi = 90$, and $\theta = 0$–360. Solid curve, TDCC-3D calculation at $b = 0.5$; dotted curve, TDCC-3D calculation at $b = 1.0$; dashed curve, TDCC-3D calculation at $b = 2.0$; dot-dashed curve, TDCC-3D calculation at $b = 4.0$ (m.a.u. = modified atomic units equal to 2.8×10^7 times atomic units such that the total cross section is in units of 1.0×10^{-24} cm^2).

then settles down into a double-peaked structure at $\theta = 90$ and $\theta = 270$ whose angle-integrated magnitude tails off at higher impact parameters. As shown in Fig. 2, the shape of the $\phi = 90$ out of plane differential cross section changes rapidly until about $b = 2.0$, then settles into a double-peaked structure at $\theta = 90$ and $\theta = 270$ whose angle-integrated magnitude is now quite small.

The differential cross section of Eq. (14) at $b = 0.10$ and $\epsilon = 6.67$ eV is shown as the dashed curve in Figs. 3 and 4
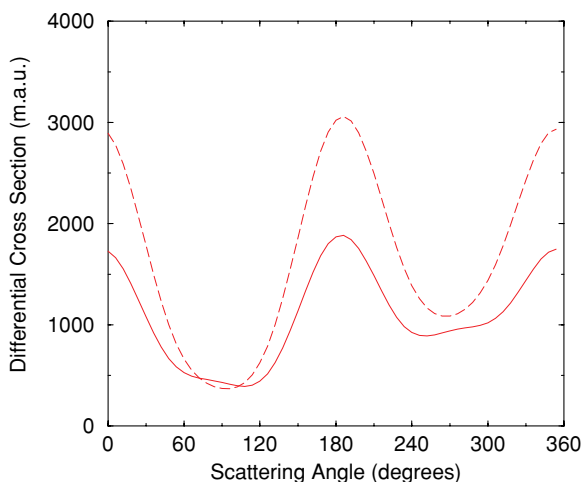

FIG. 3. (Color online) The differential cross section for single ionization in C^{6+} + He collisions at a projectile energy of 100 MeV/amu, an impact parameter of $b = 0.10$, an ejected electron energy of $\epsilon = 6.67$ eV, $\phi = 0$, and $\theta = 0$–360. Dashed curve, TDCC-3D calculation; solid curve, TDCC-6D calculation (m.a.u. = modified atomic units equal to 2.8×10^7 times atomic units such that the total cross section is in units of 1.0×10^{-24} cm^2).
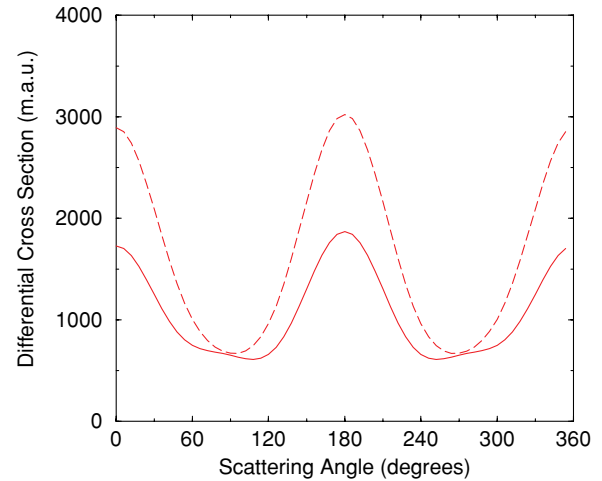

FIG. 4. (Color online) The differential cross section for single ionization in C^{6+} + He collisions at a projectile energy of 100 MeV/amu, an impact parameter of $b = 0.10$, an ejected electron energy of $\epsilon = 6.67$ eV, $\phi = 90$, and $\theta = 0$–360. Dashed curve, TDCC-3D calculation; solid curve, TDCC-6D calculation (m.a.u. = modified atomic units equal to 2.8×10^7 times atomic units such that the total cross section is in units of 1.0×10^{-24} cm^2).

for $\phi = 0$ and $\phi = 90$, respectively. For projectile motion in the xz plane as given by Eq. (8), $\phi = 0$ is the xz plane (in plane) and $\phi = 90$ is the yz plane (out of plane). Both figures have large peaks for $\theta = 0$ and $\theta = 180$ along the direction of the projectile motion. Since the mean electron radius of the He atom is $\langle r \rangle = 0.93$, a projectile at $b = 0.10$ penetrates deep enough to feel a bare ion total momentum transfer of $\Delta p = 4.0$ given by Eq. (32). For impact parameters inside the atom cloud, electrons are ejected forward and backward in regard to the projectile motion.

The differential cross section of Eq. (14) at $b = 2.4$ and $\epsilon = 6.67$ eV is shown as the dashed curve in Figs. 5 and 6 for $\phi = 0$ and $\phi = 90$, respectively. Both figures have large peaks for $\theta = 90$ and $\theta = 270$ along the direction of the projectile momentum transfer to the atom. We note that we use a spherical polar angle for θ, which is opposite in direction to the polar coordinate used in experiment [13]. Since the projectile at $b = 2.4$ is outside the atom cloud, it feels a much reduced total momentum transfer of $\Delta p < 0.01$ given by Eq. (33). For impact parameters outside the atom cloud, electrons are ejected forward and backward in regard to the projectile momentum transfer to the atom. We note that for large impact parameters that the cross-section peaks for $\phi = 0$ in plane are an order of magnitude larger than the cross-section peaks for $\phi = 90$ out of plane.

We next use the TDCC-6D method to calculate single- and double-ionization cross sections in C^{6+} + He collisions at 100 MeV/amu. On a 384×384-point uniform radial coordinate mesh with $\Delta r_1 = \Delta r_2 = 0.10$, relaxation of the TDCC-6D equations with no electron-projectile operators yields a total energy of -78.2 eV in reasonable agreement with experiment [20]. The $\hat{P}_{ll}^{00}(r_1, r_2)$ radial wave functions obtained by relaxation are used in the initial condition of Eq. (24). After setting $V_l(r) = 0$ in Eq. (10), bound orbitals are obtained by diagonalizing the radial Hamiltonian, and continuum orbitals are obtained by direct integration of the
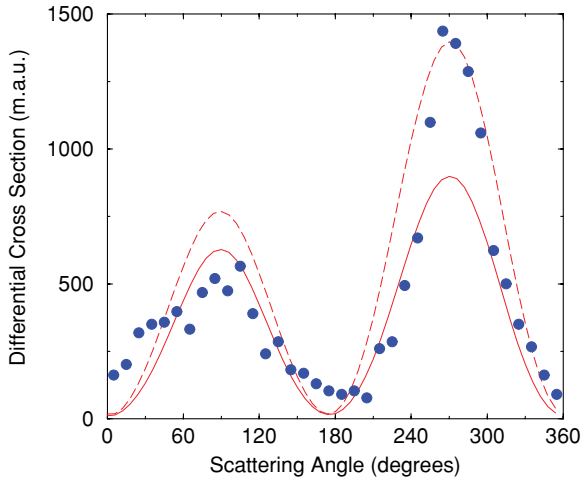
FIG. 5. (Color online) The differential cross section for single ionization in C^{6+} + He collisions at a projectile energy of 100 MeV/amu, an impact parameter of $b = 2.40$, an ejected electron energy of $\epsilon = 6.67$ eV, $\phi = 0$, and $\theta = 0$–360. Dashed curve, TDCC-3D calculation; solid curve, TDCC-6D calculation; solid circles, in-plane experiment scaled to theory (m.a.u. = modified atomic units equal to 2.8×10^7 times atomic units such that the total cross section is in units of 1.0×10^{-24} cm^2).

radial Schrödinger equation for 300 box-normalized functions with a uniform spacing of $\Delta k = 0.05$. The bound and continuum orbitals are used to obtain momentum-space wave functions in Eqs. (25) and (29).

The TDCC-6D cross-section results are obtained by time propagating Eq. (19) from $d_0 = -50$ to $d_{\text{final}} = +421$ at two different impact parameters. Both calculations used $34\, l_1 l_2 L M$ close-coupled channels. The differential cross sections of Eq. (28) for single ionization at $b = 0.10$ and $\epsilon = 6.67$ eV

are shown as the solid curve in Figs. 3 and 4. Differential cross sections at $b = 2.4$ and $\epsilon = 6.67$ eV are also shown as the solid curves in Figs. 5 and 6. The overall agreement between the TDCC-3D and TDCC-6D calculations for the single ionization differential cross sections is found to be reasonable for the general features, confirming our use of the much less computational-intensive TDCC-3D method for general trends.

We next compare our TDCC results with experiment [13]. Experimental single-ionization differential cross sections for C^{6+} + He collisions at 100 MeV/amu are reported at $\Delta p = 0.75$ and $\epsilon = 6.5$ eV for both $\phi = 0$ in plane and $\phi = 90$ out of plane. Since projectile momentum is proportional to impact parameter, scaled experimental differential cross sections in projectile momentum transfer and electron emission energy and solid angle are proportional to theoretical differential cross sections in impact parameter and electron emission energy and solid angle. A projectile momentum transfer of $\Delta p = 0.75$ yields a range of impact parameters for a process involving target ionization of $b = 0.2$ to $b = 3.5$ from Eq. (35), since there is a range of momentum transferred to the electron by the projectile which yields the specific ejected electron momentum and energy. Choosing an impact parameter near the middle of the range, the TDCC calculations for the differential cross section at $b = 2.4$, $\epsilon = 6.67$ eV, and $\phi = 0$ in plane are in reasonable agreement with the nonabsolute experimental results scaled to theory as shown in Fig. 5. In addition, the TDCC calculations for the differential cross section at $b = 2.4$, $\epsilon = 6.67$ eV, and $\phi = 90$ out of plane are also in reasonable agreement with the experimental results scaled to theory in Fig. 6. However, if we use the same scaling factor between theory and experiment as found in the in-plane case of Fig. 5, the out-of-plane experimental results are a factor of 3 higher than theory, as shown in Fig. 7. In other words, theory predicts a much larger drop in the integrated magnitude of the differential
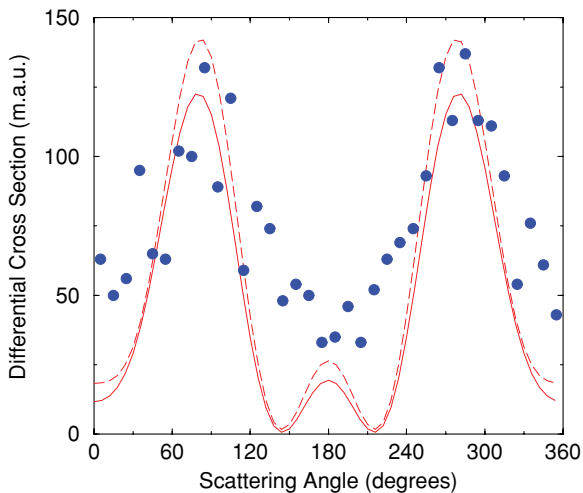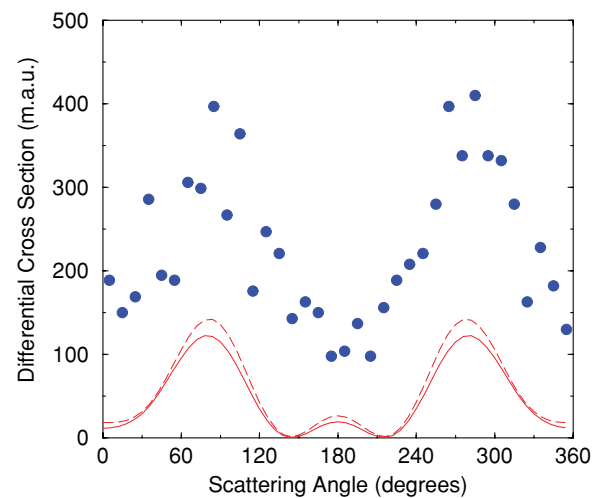

FIG. 6. (Color online) The differential cross section for single ionization in C^{6+} + He collisions at a projectile energy of 100 MeV/amu, an impact parameter of $b = 2.40$, an ejected electron energy of $\epsilon = 6.67$ eV, $\phi = 90$, and $\theta = 0$–360. Dashed curve, TDCC-3D calculation; solid curve, TDCC-6D calculation; solid circles, out-of-plane experiment scaled to theory (m.a.u. = modified atomic units equal to 2.8×10^7 times atomic units such that the total cross section is in units of 1.0×10^{-24} cm^2).

FIG. 7. (Color online) The differential cross section for single ionization in C^{6+} + He collisions at a projectile energy of 100 MeV/amu, an impact parameter of $b = 2.40$, an ejected electron energy of $\epsilon = 6.67$ eV, $\phi = 90$, and $\theta = 0$–360. Dashed curve, TDCC-3D calculation; solid curve, TDCC-6D calculation; solid circles, out-of-plane experiment scaled to theory multiplied by 3.0 (m.a.u. = modified atomic units equal to 2.8×10^7 times atomic units such that the total cross section is in units of 1.0×10^{-24} cm^2).
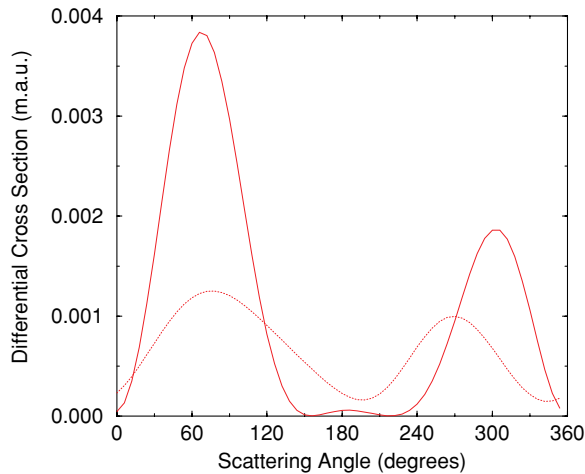
FIG. 8. (Color online) The differential cross section for double ionization in C^{6+} + He collisions at a projectile energy of 100 MeV/amu, an impact parameter of $b = 2.40$, ejected electron energies of $\epsilon_1 = \epsilon_2 = 6.67$ eV, $\phi_1 = \phi_2 = 0$, $\theta_1 = 180$, and $\theta_2 = 0$–360. Dashed curve, TDCC-6D (34 channel) calculation; solid curve, TDCC-6D (101 channel) calculation (m.a.u. = modified atomic units equal to 2.8×10^7 times atomic units such that the total cross section is in units of 1.0×10^{-24} cm^2).

cross section than experiment in going from the in-plane to out-of-plane geometry. This may be partly explained by the finite experimental resolution of the electron energies and momenta. Convoluting over the experimental uncertainties may increase the calculated cross section in this plane. We note that our comparisons are qualitatively similar to previous semiclassical calculations [21].

Finally, we present TDCC-6D results for the double ionization in C^{6+} + He collisions at 100 MeV/amu. The differential cross sections of Eq. (31) for double ionization at $b = 2.4$, $\epsilon_1 = \epsilon_2 = 6.67$ eV, $\phi_1 = \phi_2 = 0$, and $\theta_1 = 180$ are shown in Fig. 8. Calculations using both 34 $l_1 l_2 L M$ coupled channels and 101 $l_1 l_2 L M$ coupled channels find cross-section minimums for the equal-energy ejected electrons when $\theta_1 = \theta_2 = 180$ and when they are emitted back to back at $\theta_1 = 180$ and $\theta_2 = 0$. Although we find no differences in the single-ionization differential cross sections when using 34 or 101 coupled channels, there are sizable differences in the double-ionization differential cross-section peak heights. As found in the past for photon-impact and electron-impact ionization of atoms, the differential cross sections for two ejected electrons are relatively small and need a large number of coupled channels to converge on the lattice. Additional coupled channels will continue to lower the cross sections at $\theta = 0$ and $\theta = 180$, but the height of the peaks near $\theta = 30$ and $\theta = 300$ should not change that much.

IV. SUMMARY

In this article we have shown how the TDCC approach may be used to calculate fully differential cross sections in ejected electron energy and angle for single ionization of He by fast projectile impact. We have described two formulations of the TDCC approach, a 3D treatment of one active electron interacting with the projectile and a 6D treatment of two active electrons interacting with the projectile. Our 6D approach can also be straightforwardly extended to calculate the differential cross sections that arise from ion-impact double ionization of He.

For the single ionization of He by C^{6+} ions at 100 MeV/amu, the TDCC results are compared with experiment [13]. We find that for projectile-impact parameters outside the He atom charge cloud ($b > 2.0$) the TDCC results are in good qualitative agreement with measurements. In particular, we find an unequal "double-hump" shape for the in-plane-geometry differential cross sections that is in good qualitative agreement with experiment and other theories. We also find an equal double-hump shape for the out-of-plane-geometry differential cross sections that is in good qualitative agreement with experiment. However, like other theories, the TDCC results for the out-of-plane geometry case are much smaller than experiment using the original in-plane scaling factor.

In the future, we plan to develop a Fourier transform method to extract fully differential cross sections from the TDCC final time wave functions for single ionization in C^{6+} + He collisions at 100 MeV/amu. The Fourier transform method will make more precise the relative weight of the individual impact-parameter-dependent differential cross sections for a given momentum transfer to the projectile. We note that the Fourier transform method also includes an additional projectile-target ion phase factor [22]. We then plan to look at other fast ion collisions with He using different projectile ions and collision energies.

[1] M. S. Pindzola, F. Robicheaux, and J. Colgan, J. Phys. B **40**, 1695 (2007).

[2] I. F. Barna, N. Grun, and W. Scheid, Eur. Phys. J. D **25**, 239 (2003).

[3] H. Knudsen, L. H. Andersen, P. Hvelplund, G. Astner, H. Cederquist, H. Danared, L. Liljeby, and K. G. Rensfelt, J. Phys. B **17**, 3545 (1984).

[4] M. B. Shah and H. B. Gilbody, J. Phys. B **18**, 899 (1985).

[5] M. Foster, J. Colgan, and M. S. Pindzola, Phys. Rev. Lett. **100**, 033201 (2008).

[6] D. R. Schultz and P. S. Krstic, Phys. Rev. A **67**, 022712 (2003).

[7] P. Hvelplund, H. Knudsen, U. Mikkelsen, E. Moronzoni, S. P. Moller, E. Uggerhoj, and T. Worm, J. Phys. B **27**, 925 (1994).

[8] M. Foster, J. Colgan, and M. S. Pindzola, J. Phys. B **41**, 111002 (2008).

[9] M. Schulz, D. Fischer, R. Moshammer, and J. Ullrich, J. Phys. B **38**, 1363 (2005).

[10] M. S. Pindzola, J. A. Ludlow, and J. Colgan, Phys. Rev. A **80**, 032707 (2009).

[11] E. Wells, I. Ben Itzhak, K. D. Carnes, and V. Krishnamurthi, Phys. Rev. A **60**, 3734 (1999).

[12] I. Ben-Itzhak, E. Wells, D. Studanski, V. Krishnamurthi, K. D. Carnes, and H. Knudsen, J. Phys. B **34**, 1143 (2001).

[13] M. Schulz, R. Moshammer, D. Fischer, H. Kollmus, D. H. Madison, S. Jones, and J. Ullrich, Nature **422**, 48 (2003).

[14] D. Madison, M. Schulz, S. Jones, M. Foster, R. Moshammer, and J. Ullrich, J. Phys. B **35**, 3297 (2002).

[15] A. L. Harris, D. H. Madison, J. L. Peacher, M. Foster, K. Bartschat, and H. P. Saha, Phys. Rev. A **75**, 032718 (2007).

[16] M. McGovern, D. Assafrao, J. R. Mohallem, C. T. Whelan, and H. R. J. Walters, Phys. Rev. A **81**, 042704 (2010).

[17] J. Fiol, S. Otranto, and R. E. Olson, J. Phys. B **39**, L285 (2006).

[18] M. Durr, B. Najjari, M. Schulz, A. Dorn, R. Moshammer, A. B. Voitkiv, and J. Ullrich, Phys. Rev. A **75**, 062708 (2007).

[19] M. Schulz, M. Durr, B. Najjari, R. Moshammer, and J. Ullrich, Phys. Rev. A **76**, 032712 (2007).

[20] [http://physics.nist.gov/PhysRefData]

[21] F. Jarai-Szabo and L. Nagy, J. Phys. B **40**, 4259 (2007).

[22] L. Gulyas, A. Igarishi, P. D. Fainstein, and T. Kirchner, J. Phys. B **41**, 025202 (2008).